

PROPOSED SCATTERED ELECTRON DETECTOR SYSTEM AS ONE OF THE BEAM OVERLAP DIAGNOSTIC TOOLS FOR THE NEW RHIC ELECTRON LENS*

P. Thieberger[†], E. Beebe, C. Chasman, W. Fischer, D.M. Gassner, X. Gu, R. Gupta, J. Hock, R. Lambiase, C. Montag, Y. Luo, M. Minty, M. Okamura, A. Pikin, Y. Tan, J. Tuozzolo and W. Zhang

Brookhaven National Laboratory, Upton, New York, U.S.A

Abstract

An electron lens for head-on beam-beam compensation planned for RHIC requires precise overlap of the electron and proton beams which both can have down to 0.3 mm rms transverse radial widths along the 2m long interaction region. Here we describe a new diagnostic tool that is being considered to aid in the tuning and verification of this overlap. Some of the ultra relativistic protons (100 or 250 GeV) colliding with low energy electrons (2 to 10 keV) will transfer sufficient transverse momentum to cause the electrons to spiral around the magnetic guiding field in a way that will make them detectable outside of the main solenoid. Time-of-flight of the scattered electron signals will provide position-sensitive information along the overlap region. Scattering cross sections are calculated and counting rate estimates are presented as function of electron energy and detector position.

INTRODUCTION

In polarized proton operation the luminosity of RHIC is limited by the head-on beam-beam effect and methods that mitigate the effect will result in higher peak and average luminosities. Two electron lenses, one for each ring, are being constructed to partially compensate the head-on beam-beam effect in the two rings [1]. Each of these lenses consists of a low energy electron beam that creates an amplitude dependent transverse kick of the same value but opposite sign as the proton beam. The main components of the lens are the electron gun, transport solenoids and steering magnets, the superconducting main solenoid, the electron collector, beam diagnostics, power supplies and vacuum systems. The challenge of knowing that two ~0.3 mm rms wide beams are precisely overlapped, and to restore that condition when they are not is being addressed in several ways [2]. In addition to new beam position monitor systems, a bremsstrahlung detector is being developed [3] to look at radiation emitted by electrons strongly deflected by small impact parameter collisions with the highly relativistic protons, and changes in the width of the tune distribution are being considered as a diagnostic tool [4] as well as luminosity decay-rate modulation [5].

Since all of these systems have their limitations we investigate here yet another one, based on detecting energetic scattered electrons resulting from close electron-proton encounters. Such electrons will spiral along the magnetic field, and a fraction of them will thus propagate to areas external to the main solenoid where they can be detected. Potential advantages are high counting rates, fast response, relatively convenient detector location and longitudinal position discrimination. We will see below how this works in detail, but first we need to know the scattering cross section values and the energy-angle dependence of the scattered electrons.

CROSS SECTION CALCULATIONS

Describing the elastic scattering of electrons and protons (Coulomb scattering) is a two body problem that for this case of slow electrons and ultra-relativistic protons is best solved in the proton rest frame with a subsequent transformation to the lab frame. Very small angles and angular steps in the proton frame need to be chosen because the corresponding values in the laboratory are much larger. The direct calculation, namely specifying an angle in the lab and obtaining the corresponding cross section is much more difficult.

We now write the cross section in the proton frame [6]:

$$\frac{d\sigma}{d\Omega} = \frac{Z^2}{4} \left(\frac{e^2}{E}\right)^2 \frac{1}{\sin^4(\theta/2)} \left[1 - \left(\frac{pc}{E}\right)^2 \sin^2\left(\frac{\theta}{2}\right)\right] \times \left[1 + \frac{2E}{M_p c^2}\right]^{-1} \times \left[1 + \frac{q^2 \tan^2(\theta/2)}{2M_p^2}\right] \quad (1)$$

where p , E and θ are the momentum, energy and scattering angle of the electron in the proton frame. The first term corresponds to classical Rutherford scattering, the first and second bracket are respectively the quantum and recoil corrections. The last term comes from scattering off the magnetic moment of the spin $\frac{1}{2}$ proton and is small. For each of a sequence of small angles, the differential cross section is calculated with equation 1 and transformed to the rest frame using transverse momentum invariance and the equation for the invariant cross sections:

$$\left(\frac{d\sigma}{d\Omega}\right)' = \left(\frac{d\sigma}{d\Omega}\right) \times \frac{E}{E'} \times \frac{\sin^2(\theta)}{\sin^2(\theta')} \quad (2)$$

* Work supported by Brookhaven Science Associates, LLC under Contract No. DE-AC02-98CH10886 with the U.S. Department of Energy, and in part by the U.S. LHC Accelerator Research Program.

[†] PT@BNL.GOV

where the primed quantities correspond to the laboratory rest frame.

Based on these equations a computer model was implemented in EXCEL where the cross sections are converted to rates based on the beam currents, rms widths, energies and the length over which the beams overlap. Table 1 lists a set of typical input parameters for which results are shown in Figs 1-3.

Table 1: Values used to obtain the scattering rates and angle-energy dependency curves shown in Figs.1, 2, and 3.

Proton energy	250	GeV
# of bunches	111	
Protons per bunch	1E+11	
Electron energy	5.0	keV
Electron current	1.0	A
Rms beam width	0.30	mm

The proton energy used here is 250 GeV, but there will also be operation at 100 GeV. The electron energy, chosen here to be 5 keV, will range from 2 to 10 keV. As can be seen in Fig. 4, there are “bumps” or increased values of the axial magnetic field at the ends of the main solenoid, which has an otherwise uniform field. For the purposes of the halo detectors, the only effect of these magnetic field bumps (if both are present) is to prevent the electrons scattered within a certain angular range with respect to the normal from reaching the detector, as indicated by the black segments in Figs. 1, 2 and 3.

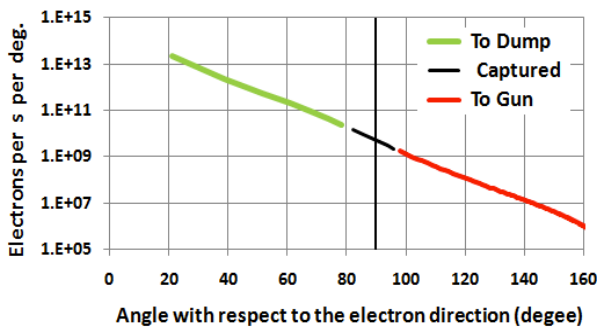


Figure 1: Number of electrons scattered per second and per degree as function of the scattering angle obtained using the parameters listed in Table 1.

We see from Fig. 1 that a large number of electrons will be scattered at small angles. Around 90 degree scattering there is a small angular range of captured electrons. And finally there is a substantial number of backscattered electrons (red segment) which, according to the results shown in Fig. 2 are the ones with the higher energies (above 132 keV for the present example). We see that the larger the backscattering angle is, the larger the energies are, but with decreasing intensities. These are the electrons of interest here. They will spiral around the magnetic field lines and return to the area close to the electron gun as will be described below.

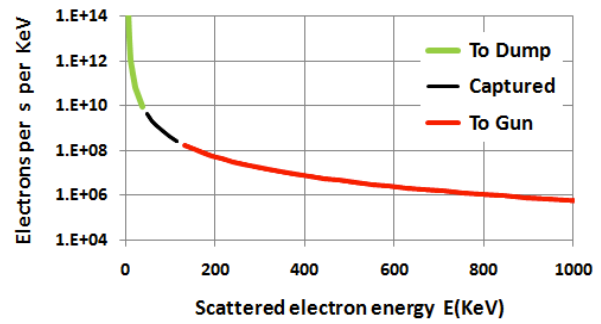


Figure 2: Number of electrons scattered per second and per keV as function of the scattering angle obtained using the parameters listed in Table 1.

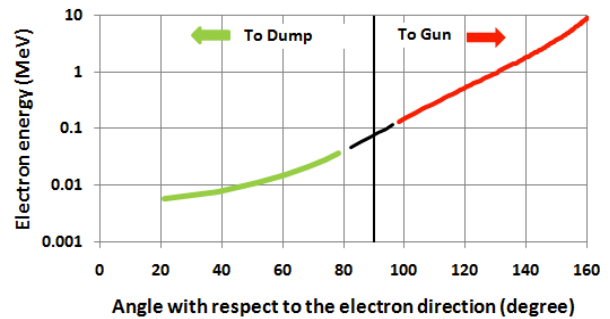


Figure 3: Scattered electron energy as function of scattering angle obtained using the parameters listed in Table 1. For ultra relativistic protons this curve is independent of proton energy.

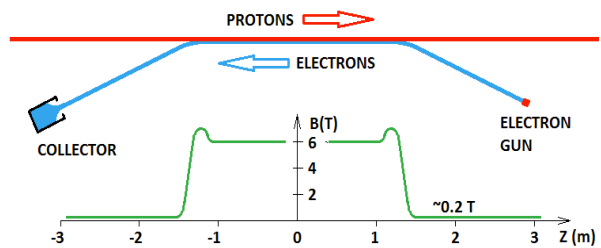


Figure 4: Schematic representation of the electron and proton trajectories and the electron gun and collector positions. This is a plan view; the electron trajectory bends occur in a horizontal plane. Also shown is the approximate shape of a typical magnetic field profile along the electron trajectory.

The dependence of the energy of the electrons on their scattering angle is shown in Fig. 3. Since this scattering process is a two body problem, there is a one-to-one correspondence as long as quantum effects are small.

ELECTRON TRACKING STUDIES

Using the backscattered electron energy-angle dependence as shown in Fig. 3, the code OPERA [7] was used to determine spiralling electron trajectories for several cases. Here we show 954 keV electrons scattered at $\pm 50.3^\circ$ (Fig. 5) and 1.5 MeV electrons scattered at $\pm 43^\circ$ (Fig. 6). In each case, the angle is chosen to correspond to

the respective energy as given by the model (Fig. 3). The trajectories are started close to the end of the main solenoid, where the field is still uniform, and propagated towards the electron gun region. Two trajectories are studied in each case, both starting in the horizontal plane with equal positive (right) and negative (left) scattering angles resulting in the projections onto a vertical plane shown in the Figs 5 and 6. Projections of all the other trajectories of electrons of these energies will fall between these two extremes, no matter where they originate along the uniform portion of the main solenoids' magnetic field. Also shown are two 5 keV electron trajectories defining the 3σ envelope of the primary electron beam propagating in the opposite direction.

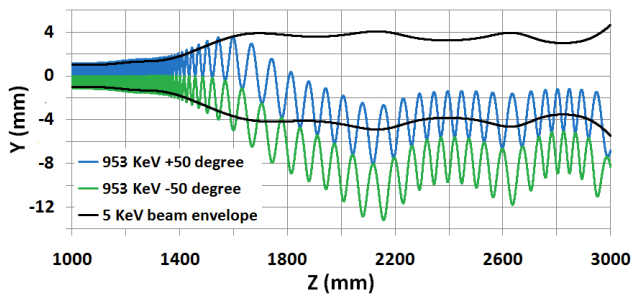


Figure 5: Tracking of electron trajectories showing the 3σ , 5 keV electron beam envelope (black), and the trajectories of 954 keV electrons scattered at +50 and -50 degrees with respect to the beam axis (blue and green respectively).

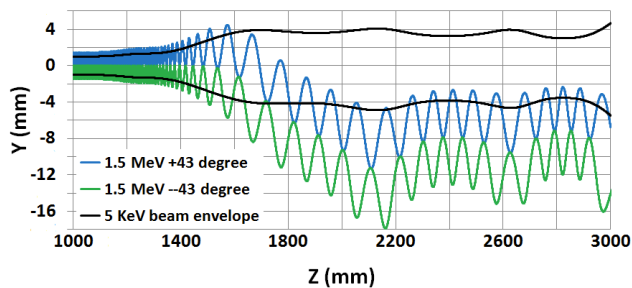


Figure 6: Tracking of electron trajectories showing the 3σ , 5 keV electron beam envelope (black), and the trajectories of 1.5 MeV electrons scattered at +43 and -43 degrees with respect to the beam axis (blue and green respectively).

An important feature observed in these trajectories is the downward drift of the spirals which is due to the horizontal bending of the magnetic field lines [8]. This displacement of the trajectories makes it possible, to locate a scattered electron detector without interfering with the primary electron beam. Comparing Figs. 5 and 6 we see that for the higher electron energies, there is better

separation between the scattered electron trajectories and the primary electron beam making it easier to place a detector. Larger separations at even higher energies could be used as well.

DISCUSSION AND CONCLUSIONS

The counting rates for the cases described in the previous sections have been roughly estimated to be $9E7/s$ and $7E7/s$ for the parameters given in Table 1, assuming that 25% and 50% of the scattered electrons of energies larger than 0.95 MeV and larger than 1.5 MeV respectively are detected. We see that even higher energy thresholds could be used. In any case, the energies are sufficiently high for the electrons to penetrate a window that is part of their shielding. A bunch intensity of $1E11$ was used here, while future bunch intensities up to $3E11$ are being considered.

There is no design yet for the detector system nor has there been a decision regarding an appropriate location. The advanced stage of the e-lens design causes changes to be challenging. Regarding the type of detector, it would be very desirable to have the individual electron energies available to be able to convert the time-of-flight information to positions along the interaction region. Silicon surface barrier or scintillation detectors could be used, but in both cases one has to face the challenge of making them compatible with the RHIC ultra high vacuum system and its baking requirements.

We have described here a possible diagnostic tool for the BNL e-lens, that could be installed in a relatively convenient location away from the main solenoid and that would satisfy the requirements of fast and accurate detection of beam-beam misalignments which is essential for tuning and for operation.

REFERENCES

- [1] W. Fischer et al., IPAC'10, p. 513 (2010).
- [2] W. Fisher, "Status of the RHIC Head-on Beam-Beam Compensation Project," these proceedings
- [3] C. Montag et al., IPAC'10, pp. 1632 (2010).
- [4] M. Minty et al.
<http://www.cadops.bnl.gov/Instrumentation/InstWiki/index.php/File:MOPEC030.pdf>
- [5] A. Valishev et al., IPAC'10, p. 2084 (2010)
- [6] F. Halzen and A. Martin, *Quarks and Leptons*, John Wiley and Sons, 1984.
- [7] Opera code, <http://www.cobham.com/home.aspx>
- [8] J. D. Jackson, *Classical Electrodynamics*, John Wiley and Sons, 1962.